

Explaining the role of vanadium in homogeneous glucose transformation reactions using NMR and EPR spectroscopy

Jakob Albert^{a,*}, Matthias Mendt^b, Michael Mozer^a, Dorothea Voß^a

^a Lehrstuhl für Chemische Reaktionstechnik, Friedrich-Alexander-Universität Erlangen-Nürnberg, Egerlandstr. 3, 91058, Erlangen, Germany

^b Felix-Bloch-Institut für Festkörperphysik, Universität Leipzig, Linnéstraße 5, 04103, Leipzig, Germany

ARTICLE INFO

Keywords:

Keggin polyoxometalates
Biomass transformation
EPR spectroscopy
NMR spectroscopy
Vanadium redox chemistry

ABSTRACT

Our contribution investigates the formation of various catalytically active vanadium species for different glucose transformation reactions. By applying both ⁵¹V-NMR (nuclear magnetic resonance) and continuous wave EPR (electron paramagnetic resonance) spectroscopy, we were able to identify the different vanadium species that catalyse glucose transformation to several organic acids in aqueous solution depending on the reaction atmosphere and type of vanadium precursor. Under aerobic conditions (20 bar oxygen atmosphere) we could prove that only the higher-substituted vanadium containing polyoxometalate HPA-5 (H₈PV₅Mo₇O₄₀) catalyses the desired glucose oxidation to formic acid at 90 °C. Moreover, our results suggest that substituted V⁵⁺ species are the predominantly catalytic active species in the production of formic acid. Using anaerobic conditions (20 bar nitrogen atmosphere), we could show that different vanadium species are formed depending on the nature of the precursor. Hereby, paramagnetic acid-bound vanadyl species formed from the VOSO₄ and NH₄VO₃ as well as the HPA-5 precursor seem to be predominantly responsible for lactic acid formation from glucose under anaerobic conditions.

1. Introduction

Catalytic oxidation chemistry of biomass is gaining both scientific and industrial interest. Hereby, several pretreatment steps are required before direct chemical valorisation is possible. The main effort is to overcome the recalcitrant nature of the water-insoluble feedstock by acid-catalysed depolymerisation followed by oxidative cleavage of the carbon bonds in the biomass framework [1,2].

Lignocellulosic biomass as the most abundant class of biogenic materials typically contains more than 50 wt% sugars that can be upgraded to valuable platform chemicals [3]. Lignocellulose consists of the three main components cellulose (ca. 50%), hemicellulose (25–30%) and lignin (15–25%) [4]. The aromatic lignin is the most underutilized fraction. It has been traditionally employed for heat and power purposes through combustion in the pulp and paper industry due to its high caloric value [5]. Hemicellulose mainly contains C₅ sugars like xylose or arabinose having important applications for biofuel production (e.g. bioethanol) and for the generation of valuable chemical intermediates (e.g. furfural) [6]. Cellulose is comparably considered as one of the most abundant biopolymers on earth comprising linear β(1,4) glucose C₆-chain links [7]. Furthermore, the latter can be converted into valuable products such as biofuels (e.g. bioethanol) and

platform chemicals like levulinic acid (LevA), formic acid (FA), gamma-valerolactone (GVL) and derived products like several oxygenates [8–10].

The reaction sequence for valorisation of lignocellulose starts with the fractionation of the main components followed by acid-catalysed hydrolysis of cellulose and hemicellulose into water-soluble monosaccharides such as glucose, fructose, or xylose and the subsequent oxidative cleavage of C–C bonds in monosaccharides into low-molecular carboxylic acids like FA [11], acetic acid (AA) [12,13] or lactic acid (LA) [14].

Over-oxidation of the monosaccharides and intermediates results in the thermodynamically favored complete combustion to carbon dioxide and water [15]. Consequently, it is of critical importance that the applied catalyst systems prevent total oxidation leading to CO₂ but catalyze partial oxidation leading to FA [16]. Moreover, in the context of a sustainable chemical transformation of biomass, only environmentally friendly reagents such as water (solvent) or molecular oxygen (oxidizing agent) should be used [17].

The required oxidative carbon-carbon bond cleavage by using molecular oxygen (O₂) in aqueous media can be accomplished by several metal catalysts [18–20]. In particular, V-containing catalysts such as polyoxometalates (POMs) [21–23] and water-soluble vanadium

* Corresponding author.

E-mail address: jakob.albert@fau.de (J. Albert).

<https://doi.org/10.1016/j.apcata.2018.10.030>

Received 29 August 2018; Received in revised form 17 October 2018; Accepted 23 October 2018

Available online 30 November 2018

0926-860X/ © 2018 Elsevier B.V. All rights reserved.

precursors such as NaVO_3 [24] or VOSO_4 [14,25] can effectively catalyze this transformation.

POMs are well-defined metal-oxyanions linked with oxygen bridges of early transition metals at their highest oxidation state (e.g. Mo^{6+} , W^{6+} or V^{5+}). They can also contain a multitude of hetero atoms to improve their chemical and thermal stability [26]. POMs reveal unique physical and chemical properties like tunable acid-base properties, great redox activity based on the fast and reversible multielectron transfer, high thermal stability and excellent solubility and stability in water [27,28].

Mostly used in homogeneous catalyzed oxidation reactions are POMs from the so called Keggin-type $[\text{XM}_{12}\text{O}_{40}]^{n-}$. They contain a template of various coordinating anions, e.g. oxoanions, oxometalates or halides, together with a framework metal which is typically an early, high-valent transition metal [29,30]. The catalytic activity is mostly introduced by substituting some of the framework metals (W, Mo) with easily reducible heterometals like vanadium that results in shifting their reactivity from acidic to redox-dominance [31]. The generated compounds have the composition $\text{H}_{3+n}[\text{PV}_n\text{Mo}_{12-n}\text{O}_{40}]$ and are called heteropolyacids, abbreviated as HPA-n depending on the content of vanadium atoms (n) and have proven to be the most efficient biomass oxidation catalysts in aqueous solution [32,33].

In 2011, some of us developed the selective oxidation of biomass to formic acid (OxFA process) using the above mentioned homogeneous POM catalysts [34,35]. By modifying both the process conditions and the chemical composition of the catalyst, we were able to expand the raw material base on complex, water-insoluble biomass of different origin and composition. Furthermore, a systematic study of the re-oxidation behavior of the homogeneous POM catalyst in aqueous solution together with an optimisation of the catalyst synthesis lead to a superior performance concerning lower oxygen pressures and faster reaction kinetics [36].

Nuclear magnetic resonance (NMR) and electron paramagnetic resonance (EPR) spectroscopy methods are very powerful tools to identify various V^{5+} as well as V^{4+} species in solution. The ^{51}V nuclear isotope occurs in a natural abundance of almost 100% and has a nuclear spin of $I = 7/2$. Furthermore, the V^{5+} ion is diamagnetic since it has a closed shell $3p^6$ electron configuration. Therefore, NMR is an ideal tool for the detection of various V^{5+} species in aqueous solution. It resolves only the isotropic chemical shift, whereas the chemical shift anisotropy as well as the first-order nuclear quadrupole coupling average to zero due to the rapid tumbling of the molecules [37]. Nevertheless, the isotropic chemical shift of V^{5+} species is highly informative since it significantly depends on the local electronic environment and is therefore a fingerprint for a certain V^{5+} species.

EPR cannot detect V^{5+} species due to their diamagnetism but can measure characteristic signals of V^{4+} species, since V^{4+} has a $3d^1$ electron configuration and therefore an electron spin $S = 1/2$. Thus, one usually cannot detect NMR signals of V^{4+} species due to the fast magnetically induced nuclear relaxation [38]. In this sense, NMR and EPR complement each other. Two magnetic interactions define predominantly the signal of a V^{4+} species, measured by EPR in continuous wave (CW) mode. The electron Zeeman interaction describes the interaction between the unpaired electron and the external magnetic field and is described by the so called dimensionless g-tensor, which is the EPR equivalent of the chemical shift tensor in NMR. In liquids the g-tensor anisotropy is likewise averaged out so that liquid EPR usually resolves only the isotropic g-value g_{iso} which is for V^{4+} near but slightly smaller than the free electron g-value $g_e = 2.0023$. Liquid EPR of V^{4+} species also resolves the isotropic hyperfine interaction (hfi) between the unpaired electron and the ^{51}V nucleus spin $I = 7/2$, which leads to a characteristic splitting of the EPR spectrum into eight hfi transitions. Again, the hfi anisotropy is almost averaged out by the fast tumbling of the molecule. Nevertheless, in the fast motion regime, which applies for the present V^{4+} species in aqueous solution, the hfi anisotropy as well as the rotational correlation time τ_c still determine to some extend the

line widths of each hfi transition [39]. Here least square fitting routines are very helpful for reproducing their exact line shapes. Unfortunately, the effects of τ_c and the hfi-anisotropy stand in such a certain mutual relationship, that a unique determination of both from fast motion EPR spectra of V^{4+} species alone is not possible without knowing at least one of both quantities. Therefore one has to set one parameter to a certain but arbitrary value, using the second as a fitting parameter. Nevertheless, the isotropic g-value and isotropic hfi parameter alone provide valuable information since they likewise are characteristic for specific V^{4+} species.

In this contribution, we wanted to clarify the role of different vanadium species from several precursors (simple vanadium salts as well as heteropolyacids) for the transformation of glucose under aerobic (O_2 -atmosphere) or anaerobic (N_2 -atmosphere) conditions in aqueous media by applying both NMR and EPR spectroscopy. This allows for a deeper understanding of biomass transformation processes. Herein, we used two commercially available water-soluble vanadium sources, one containing initially V^{5+} (NH_4VO_3) and one containing initially V^{4+} (VOSO_4) in order to identify the different catalytically active vanadium species under reaction conditions. Thereby, it is known that formation of various carboxylic acids like FA or LA from glucose is dependent on the reaction atmosphere [14,34]. Moreover, two heteropolyacids, namely $\text{H}_4\text{PV}_1\text{Mo}_{11}\text{O}_{40}$ (HPA-1) and $\text{H}_8\text{PV}_5\text{Mo}_7\text{O}_{40}$ (HPA-5) containing different amounts of vanadium were also tested for the catalytic transformation of glucose under aerobic or anaerobic conditions.

2. Experimental

2.1. Materials

All reagents and substrates were commercially available and used as received. The model substrate glucose was supplied by Merck KGaA with a purity of 99.5%. The vanadium precursor NH_4VO_3 was purchased from Acros Organics with a purity of 99.5%. VOSO_4 was obtained from Alfa Aesar with a purity of 99.9%. The catalysts HPA-1 ($\text{H}_4\text{PVMo}_{11}\text{O}_{40}$) and HPA-5 ($\text{H}_8\text{PV}_5\text{Mo}_7\text{O}_{40}$) were both synthesized according to the literature [16,40]. The characterization of the catalysts has been carried out using a Perkin Elmer Plasma 400 ICP-OES device resulting in a P/V/Mo ratio of 1/0.82/11.14 for HPA-1 and 1/4.80/6.93 for HPA-5, respectively. Oxygen (4.5 GA 201) and Nitrogen (5.0) were bought from Linde AG. Demineralized water was used as a solvent for all experiments.

2.2. Catalytic transformation reactions (results of Tables 1 and 2)

The catalytic transformation reactions were carried out in a tenfold screening plant with a batch mode reactor setup. It consists of ten 20 mL autoclaves out of Hastelloy C276. All pipes, valves and fittings were made of stainless steel 1.4571. The gaskets used were made of Teflon. The autoclaves were connected in parallel to a single oxygen supply line via individual couplings and placed inside a heating plate in order to adjust the required temperature. The heating plate was equipped with a magnetic stirrer whereby magnetic stirrer bars could be used for stirring. Additionally, each reactor was connected to a rupture disk with a burst pressure maximum of 90 bar.

2.3. Typical work-up procedure

For the catalytic transformation reactions, each autoclave was filled with 1 mmol glucose (0.18 g), 0.1 mmol catalyst and 10 g water as the solvent. The system was purged with 10 bar pure oxygen or nitrogen in order to remove the residual air out of the reactors. Afterwards, the reactors were pre-pressurized with about 16 bar, the stirrer was set to 300 rpm and the heating was switched on. When the desired temperature (90 °C under O_2 -pressure respectively 90 °C or 160 °C under N_2 -pressure) was reached, the pressure was increased to the required

pressure of 20 bar and the stirring speed was set to 1000 rpm in order to start the gas entrainment. This moment was set as starting time of the experiment.

2.4. Determination of quantitative reaction parameters

After the reactions all products were quantitatively determined by HPLC- and GC-analysis. The yields of FA, AA, LA, LevA and HMF were determined by means of HPLC measurements using a HPLC from Jasco equipped with a 300 mm x 8 mm SH1011 Shodex column and calculated as $n(\text{product})/n(\text{C-atoms glucose})$. The yields of CO_2 were determined by means of GC-analysis using a Varian GC 450 equipped with a 2 m x 0.75 mm ID ShinCarbon ST column and calculated as $n(\text{CO}_2)/n(\text{C-atoms glucose})$. No other gaseous products could be detected by the used GC.

2.5. Nuclear magnetic resonance (NMR) spectroscopy

The NMR spectra were recorded on a Jeol ECX-400 MHz spectrometer (9.4 T) at 293 K. The ^{51}V NMR spectra were measured with 2024 scans in a range of -580 to -460 ppm with an excitation frequency of 105.25 MHz and a resolution of 0.77 Hz. The field frequency stabilization was locked to deuterium by placing a coaxial inner tube with D_2O into a 10 mm tube containing the sample.

2.6. Electron paramagnetic resonance (EPR) spectroscopy

Continuous wave EPR spectra of the liquid samples were measured at room temperature at X-band frequency (9.5 GHz) using a rectangular Varian resonator and special flat quartz glass tubes to avoid dielectric losses by the water molecules enabling the coupling of the microwave (mw) to the resonator. The liquid samples were pipetted into such a cell, filling the same volume during the EPR measurements in all cases with an estimated error of 5%. All experimental EPR spectra were normalized with respect to the number of scans and where otherwise conducted with the same experimental parameters, including a microwave power of 20 mW, a modulation frequency of 100 kHz and a modulation amplitude of 1 m T. Before each measurement of a single sample, the quality (Q) factor was measured and the presented signals were also normalized with respect to it. The spectra were measured on two different days. The first day the Q-factor was about 2000 and the second day about 1000. But a same VOSO_4 sample before the reaction was measured on both days as a reference. Its normalized EPR signal intensities, considering the Q-factor, were exactly the same for measurements on both days, verifying that the measurement conditions were reproducible and that the experimental derived EPR intensities are comparable.

EPR signals of the V^{4+} species were analyzed using the MatLab toolbox EasySpin version 5.2.20 [53]. Before their simulations they were base line corrected by third order polynomials. All signals were fitted by simulated EPR signals of one or the sum of two V^{4+} species using the EasySpin function `garlic` for isotropic fast motional EPR spectra and a

least square routine implemented by the MatLab R2017a optimization toolbox, allowing fits with high precision. The fitting parameters for the simulations of each species were the isotropic g-value g_{iso} , the isotropic ^{51}V hfi parameter A_{iso} , two phenomenological isotropic convolutional Gaussian and Lorentzian line width parameters, the base-10 logarithm of the rotational correlation time for isotropic rotational diffusion, the total intensity of the simulated signal as well as the relative amount of the second species, if considered. The anisotropies of the g- and hfi tensors are not resolved but were set to typical values $\frac{g_{\parallel} - g_{\perp}}{3} = -0.014$ [48] and $\frac{A_{\parallel} - A_{\perp}}{3} = 111.5$ MHz [50] assuming axial symmetric g- and hfi tensors. Here g_{\parallel} and g_{\perp} are the principle values of the g-tensor in z-direction and in the x,y-plane, as A_{\parallel} and A_{\perp} are for the ^{51}V hfi tensor. Note that a large range of such g- and hfi-tensor anisotropy is consistent to the experimental signals depending on the correlation time. Therefore in the present study the latter was used only as a fitting parameter. Corresponding values are given in the ESI, part 4. The errors of the parameters were estimated by varying the corresponding parameter around the best fit of the simulated signal.

The experimental intensities of the normalized EPR spectra were calculated by the double integration of the spectra, after third order polynomial base line corrections before each integration step.

3. Results and discussion

3.1. Catalytic glucose oxidation using various V-sources under aerobic conditions

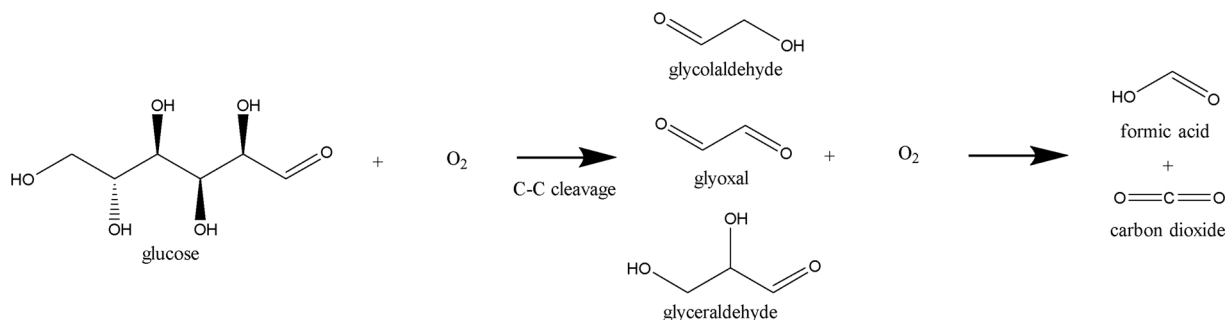
In the first set of experiments, we chose the well-known glucose oxidation reaction under O_2 atmosphere (based on former studies) [8,56] to investigate the effects of free vanadium in solution. Therefore, we chose VOSO_4 as a source for paramagnetic V^{4+} and NH_4VO_3 as a source for diamagnetic V^{5+} in comparison to vanadium-ions bound in a three-dimensional network like the Keggin-POM structures HPA-1 and HPA-5 for their oxidation ability under aerobic conditions. The chosen reaction conditions were comparable to those of the classical OxFA process [11,34].

Scheme 1 shows the main reaction pathway from glucose to formic acid suggested by Wölfel et al. [8] and Li et al. [56] under aerobic conditions catalyzed by a HPA-2 catalyst.

The experiments were carried out in a tenfold screening plant with a batch mode reactor setup consisting of ten 20 mL autoclaves. Each reactor was filled with 1 mmol glucose (0.18 g), 0.1 mmol catalyst and 10 g demineralized water as the solvent. The catalytic transformation reactions were performed under 20 bar oxygen pressure at 90 °C using 1000 rpm for 3 h reaction time in order to study the initial kinetic regime.

Table 1 shows the results of the screening of the four different vanadium sources under aerobic conditions.

Using a reaction time of 3 h, we could demonstrate that only the HPA-5 catalyst shows a good activity for glucose oxidation ($X = 42.9\%$) under aerobic conditions without the help of any additives like acidity



Scheme 1. Main reaction steps for vanadium-catalyzed glucose oxidation in aqueous solution under aerobic conditions [56].

Table 1
Screening of different vanadium precursors for the reaction with glucose under O₂-atmosphere in aqueous solution.

Entry	Catalyst	Conversion [%]	Yield ^a FA [%]	Yield CO ₂ [%]	pH-value before [-]	pH-value after [-]
1	VOSO ₄	3.4	2.7	0.7	3.3	2.1
2	NH ₄ VO ₃	2.8	2.0	0.7	6.7	3.0
3	HPA-1	0.2	< 0.1	0.2	1.5	1.5
4	HPA-5	42.9	34.3	8.6	1.8	1.6

Reaction conditions: 1 mmol glucose, 0.1 mmol catalyst dissolved in 10 g H₂O, 20 bar O₂, 90 °C, 3 h, 1000 rpm; Conversion, yields and selectivities determined as described in the corresponding section of the experimental part. ^a Neither AA, LA, LevA or HMF could be detected under these conditions.

promoters (sulfuric acid [22], para-toluenesulfonic acid [34]) or co-oxidants like FeCl₃ [15]. Under mild oxidation temperatures of 90 °C, a moderate conversion of glucose resulting in a FA-yield of 34% with an outstanding liquid-phase selectivity of > 99% (proven by HPLC measurements) was reached. CO₂ was the only byproduct in the gas phase (Y_{CO₂} = 8.6%) resulting from the competing total oxidation pathway of glucose to carbon dioxide and water [8]. Interestingly, former publications claimed that simple vanadium precursors like NaVO₃ and VOSO₄ should also be suitable oxidation catalysts for carbohydrates like glucose under oxidative conditions [12,24]. However, the simple V⁵⁺ source NH₄VO₃ as well as the commercial V⁴⁺ source VOSO₄ both showed the same poor activity with only around 3% glucose conversion after 3 h reaction time. One possible explanation for this diverse behavior could be found in literature, where the presence of different vanadium species is linked to the pH value in aqueous solution [40,41]. Interestingly, the pH using the HPA-5 drops only slightly from 1.8 to 1.6 although FA was formed. However, the same effect can be observed using VOSO₄ where the pH drops from 3.3 to 2.1 without significant FA formation indicating a change in the nature of the vanadium species. Regarding NH₄VO₃, there was a very drastic change from almost neutral (6.7) before reaction down to 3.3 after reaction without significant FA formation. Finally, the HPA-1 heteropolyacid did not show any catalytic activity under the applied reaction conditions as only traces of FA could be detected by the used HPLC analysis. The pH also remains constant indicating no change in the nature of the vanadium species. Therefore, we exclude pH effects being the only reason for forming a catalytic active vanadium species under the applied reaction conditions.

In order to clarify these findings and to investigate the nature of the applied vanadium species, we performed both ⁵¹V-NMR and EPR-spectroscopy measurements before and after the reaction, as it is well-known that V-O species in aqueous solution undergo certain dissociation reactions depending on the pH-level of the solution [40–42]. In redox catalysis, the vanadium–oxygen (V–O) species are firstly reduced by the substrate and then oxidized by an oxidant under aerobic conditions to complete a catalytic cycle, or the vanadium–oxygen species activates the oxidant to form an intermediate that oxidizes the reactants [42]. The selectivity of the products is highly dependent on the V–O species present in these reactions depending on the oxidation state of vanadium in aqueous solution.

First, we want to admit that for all respective samples we cannot exclude the presence of distinct V³⁺ species [43]. V³⁺ has a 3d² electron configuration and has therefore an electron spin *S* = 1. Since it is paramagnetic, its detection by NMR should fail. Moreover, since it has an integer electron spin, no allowed EPR transition can be excited by the applied microwave frequency (≈ 9.5 GHz), if the zero field splitting is larger than 30 GHz, as spectral simulations suggest. For a V³⁺ hexaqua cation, a zero field splitting of about 143 GHz was determined by high-field multifrequency EPR [44]. Thus we expect that a significant presence of V³⁺ in the various aqueous solutions cannot ruled out or

confirmed neither by NMR nor EPR [45].

Experimental and simulated room temperature EPR signals of the VOSO₄ sample before the reaction in combination with ⁵¹V-NMR measurements confirmed that exclusively one paramagnetic V⁴⁺ species is present (see ESI, Figure S1) whereas no V⁵⁺ species is present within the sensitivity of NMR (see ESI, Figure S2). More specifically, EPR detects before the reaction a single V⁴⁺ species A_{VOSO₄} with an isotropic g-value g_{iso} = 1.9638 ± 0.001 and an isotropic ⁵¹V hyperfine interaction (hfi) value of A_{iso} = 317.5 ± 2 MHz (see ESI, Table S1), which can be assigned to vanadyl (VO²⁺) in the form of [V⁴⁺O(H₂O)₅]²⁺ [48,49]. After the reaction under aerobic conditions at 90 °C for 3 h, the same vanadyl species A_{VOSO₄} was predominantly found using EPR spectroscopy (see ESI, Figure S9 and Table S1). However, its EPR derived amount has decreased to about 22% of its amount before the reaction (see ESI, Table S1). Moreover, NMR detects a new peak with a chemical shift at -543 ppm, which is attributable to a VO₂⁺ species in aqueous solution (see ESI, Figure S10) leading to a decreasing pH level [14,46]. Obviously, the oxidation of some V⁴⁺-ions to V⁵⁺ in the form of VO₂⁺ did not lead to a significant catalytic oxidation of glucose to FA under the applied reaction conditions. Therefore, we claim that VOSO₄ is not a suitable catalyst for low-temperature biomass oxidation below 100 °C.

Using NH₄VO₃ as vanadium source did also not lead to a noteworthy catalytic oxidation activity (see Table 1), although ⁵¹V-NMR and EPR measurements confirm that all initial vanadium before the reaction is present as V⁵⁺ in the form of VO₃⁻ (see ESI, Figure S3 and Figure S4). According to Hayashi et al. [47], the dominant signal in the ⁵¹V-NMR spectrum at -578 ppm can be assigned to α-NH₄VO₃ whereby the two minor peaks at -558 ppm and -572 ppm refer to impurities like KVO₃ and NaVO₃, respectively (see ESI, Figure S4). After the reaction, three peaks are observable in the ⁵¹V-NMR spectra corresponding to the decavanadate species [H₂V₁₀O₂₈]⁴⁻ (see ESI, Figure S12) [42,46]. Obviously, vanadium in the V⁵⁺O₃- precursor does not undergo a transformation to V⁵⁺O₂⁺ under the applied oxidative conditions which is supposed to happen at the pH level of 3.3 [41]. Additionally, contributions of two different V⁴⁺ species A_{NH₄VO₃} and B_{NH₄VO₃} can be resolved by EPR after the reaction (see ESI, Figure S11). Within the spectral resolution, the isotropic spin Hamiltonian parameters of species A_{NH₄VO₃} almost equals those of species A_{VOSO₄} (see ESI, Tables S1 and S2). We therefore attribute tentatively this species to [V⁴⁺O(H₂O)₅]²⁺, too [48,49]. For species B_{NH₄VO₃} one derives by spectral simulations the parameters g_{iso} = 1.9657 ± 0.002 and A_{iso} = 296.5 ± 2 MHz (see ESI, Table S2). This species can probably be attributed to an acid-bound vanadyl complex, presumably [V⁴⁺O(COOH)₂]²⁺ [49,52]. The small amounts of both vanadyl species (see ESI, Table S2) indicate that only a small fraction of VO₃⁻ is reduced. Relying on these results, one can exclude that VO₃⁻ leads to a significant catalytic oxidation of glucose to FA under the applied reaction conditions.

Regarding the HPA-1 heteropolyacid, small contributions of two different V⁴⁺ species A_{HPA1} and B_{HPA1} are resolved by EPR before the reaction (see ESI, Figure S5). Due to its isotropic spin Hamiltonian parameters g_{iso} = 1.9639 ± 0.001 and A_{iso} = 318.1 ± 2 MHz the former can be attributed again to [V⁴⁺O(H₂O)₅]²⁺ [48,49]. For the latter, parameters g_{iso} = 1.9635 ± 0.002 and A_{iso} = 250.4 ± 8 MHz have been derived (see ESI, Table S3). They almost equal those of the V⁴⁺ species in ammonium [50] and cesium [54] salts of [PVMo₁₁O₄₀]⁴⁻. As it was indicated by EPR, the corresponding V⁴⁺ species are not incorporated at a Mo site [54]. Structures have been proposed, where a VO²⁺ species rather coordinates to three or four oxygens at the outer surface of the Keggin molecule [54,55]. Consequently, we tentatively assign species B_{HPA1} to VO²⁺, coordinating to the outer surface of a [PV⁵⁺Mo₁₁O₄₀]⁴⁻ heteropolyanion. Moreover, the ⁵¹V-NMR spectrum shows V⁵⁺ present as only one distinct peak referring to the single isomer [PV⁵⁺Mo₁₁O₄₀]⁴⁻ according to the literature (see ESI, Figure S6) [43]. After the applied reaction time of 3 h under oxidative conditions, the same two paramagnetic V⁴⁺ species can be

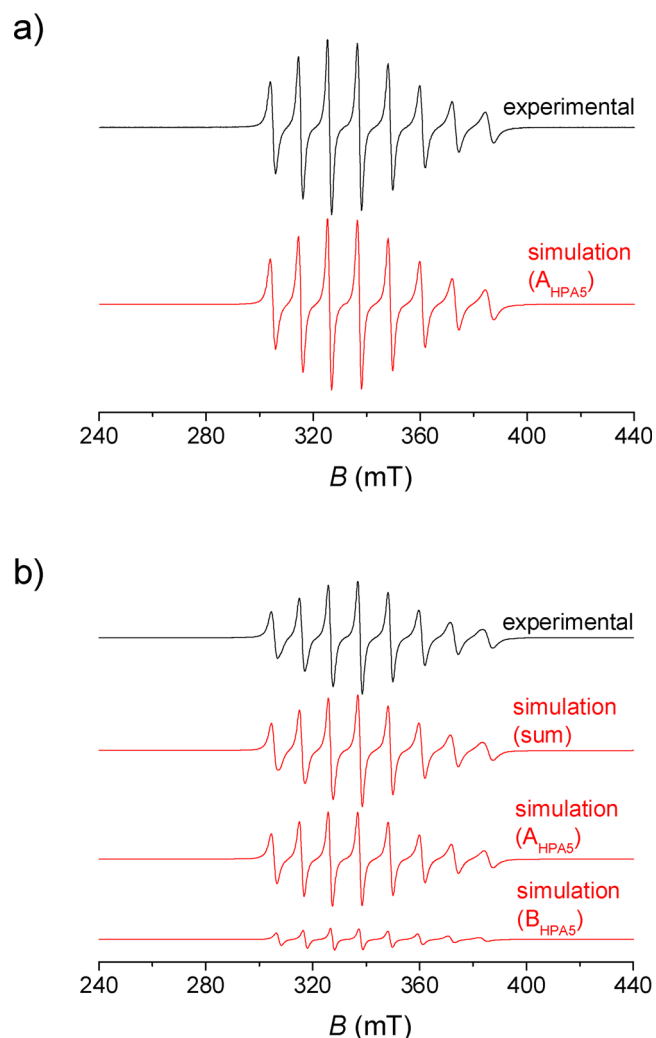


Fig. 1. Experimental (black) and simulated (red) EPR spectra of the 0.1 mmol HPA-5 solution before (a) and after (b) the reaction with glucose under aerobic conditions. The EPR signal before the reaction (a) can be simulated by a single species A_{HPA5} as indicated in the figure. After the reaction (b) the simulated EPR signal (sum) is a superposition of the simulated signals of species A_{HPA5} and species B_{HPA5} as indicated in the figure (For interpretation of the references to colour in this figure legend, the reader is referred to the web version of this article).

detected by EPR (see ESI, Figure S13, and Table S3) as well as the same $[\text{PV}^{5+}\text{Mo}_{11}\text{O}_{40}]^{4-}$ diamagnetic species was visible using ^{51}V -NMR spectroscopy (see ESI, Figure S14). Interestingly, the amount of species B_{HPA1} slightly increases during the reaction (see ESI, Table S3), indicating the reduction of some $[\text{PV}^{5+}\text{Mo}_{11}\text{O}_{40}]^{4-}$ to $[\text{PV}^{4+}\text{Mo}_{11}\text{O}_{40}]^{5-}$. However, the results clearly demonstrate that the HPA-1 precursor is not catalytically active under the applied reaction conditions.

For the active HPA-5 catalyst, interestingly a comparably large amount of vanadium is present as paramagnetic V^{4+} (29% relative to the amount of V^{4+} in the VOSO_4 sample before the reaction, see ESI, Table S4), whereby one species A_{HPA5} could be detected by EPR prior to the reaction identified again by its isotropic spin Hamiltonian parameters as $[\text{V}^{4+}\text{O}(\text{H}_2\text{O})_5]^{2+}$ (see Fig. 1 and ESI, Table S4) [48,49]. After the reaction, the amount of this species has been decreased significantly to 8% (see ESI, Table S4), indicating the oxidation of most V^{4+} to various V^{5+} species. In addition, EPR resolves the minor presence of a second V^{4+} species B_{HPA5} after the reaction (see Fig. 1), which can be attributed again to acid-bound vanadyl, presumably $[\text{V}^{4+}\text{O}(\text{COOH})_2]$ (see ESI, Table S4) [49,52]. However, a large amount of vanadium is

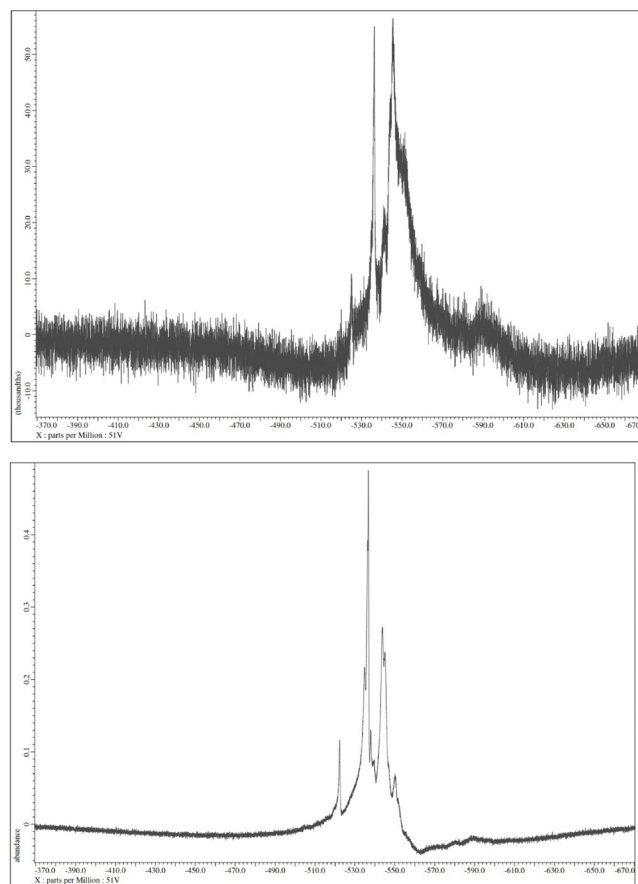
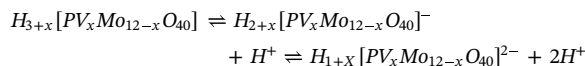


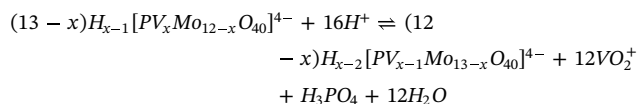
Fig. 2. ^{51}V -NMR spectra of the 0.1 mmol HPA-5 solution before (top) and after (bottom) the reaction with glucose under aerobic conditions.

present as V^{5+} before and after the reaction, as can be seen in the corresponding ^{51}V -NMR spectra (see Fig. 2). As already known from the literature, aqueous HPA-5 solution is a complex mixture of different species and isomers because of different equilibrium reactions of V-Mo-P-substituted heteropolyacids in aqueous solution (see Scheme 2) [51].

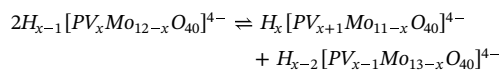
- acid-base equilibrium for all HPA- x ($x = 1-6$):



- protolysis in strong acidic media for HPA- x ($x > 1$):



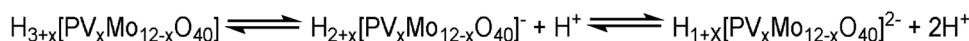
- disproportionation reaction for HPA- x ($x > 2$):



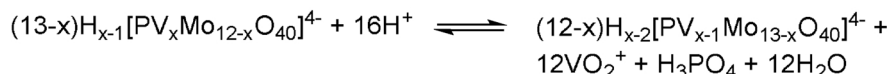
Consequently, aqueous solutions of HPA-5 contain not only $\text{H}_8\text{PV}_5\text{Mo}_7\text{O}_{40}$ itself but also lower and higher V-substituted Keggin species such as $\text{H}_9\text{PV}_6\text{Mo}_6\text{O}_{40}$ (HPA-6), $\text{H}_7\text{PV}_4\text{Mo}_8\text{O}_{40}$ (HPA-4), $\text{H}_6\text{PV}_3\text{Mo}_9\text{O}_{40}$ (HPA-3), $\text{H}_5\text{PV}_2\text{Mo}_{10}\text{O}_{40}$ (HPA-2), $\text{H}_4\text{PV}_1\text{Mo}_{11}\text{O}_{40}$ (HPA-1), as well as VO_2^+ , H_3PO_4 and $\text{H}_3\text{PMo}_{12}\text{O}_{40}$ (HPA-0). Therefore, different isomers depending on the degree of V-substitution in the Keggin structure are possible [42,51].

Figs. 1 and 2 show a comparison of the EPR and ^{51}V -NMR spectra before and after the reaction with glucose under aerobic conditions for

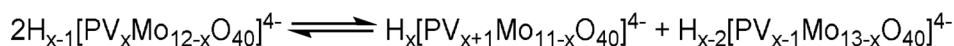
- acid-base equilibrium for all HPA-x (x=1-6):



- protolysis in strong acidic media for HPA-x (x>1):



- disproportionation reaction for HPA-x (x>2):



Scheme 2. Different equilibrium reactions of HPA-x in aqueous solution [51].

Table 2

Summary of the different vanadium species resulting from the reaction with glucose under aerobic conditions determined by EPR and NMR spectroscopy.

Entry	Catalyst	V ⁴⁺ Species before reaction under O ₂ ^a	V ⁴⁺ Species after reaction under O ₂ ^a	V ⁵⁺ Species before reaction under O ₂ ^b	V ⁵⁺ Species after reaction under O ₂ ^b
1	VOSO ₄	[V ⁴⁺ O(H ₂ O) ₅] ²⁺	[V ⁴⁺ O(H ₂ O) ₅] ²⁺	–	[V ⁵⁺ O ₂] ⁺
2	NH ₄ VO ₃	–	[V ⁴⁺ O(H ₂ O) ₅] ²⁺ [V ⁴⁺ O(COOH) ₂]	[V ⁵⁺ O ₃] [–]	[H ₂ V ₁₀ O ₂₈] ^{4–}
3	HPA-1	[V ⁴⁺ O(H ₂ O) ₅] ²⁺ VO ₂ ⁺ @ [PV ⁵⁺ Mo ₁₁ O ₄₀] ^{4–}	[V ⁴⁺ O(H ₂ O) ₅] ²⁺ VO ₂ ⁺ @ [PV ⁵⁺ Mo ₁₁ O ₄₀] ^{4–}	[H ₁ PVMo ₁₁ O ₄₀] ^{3–}	[H ₁ PVMo ₁₁ O ₄₀] ^{3–}
4	HPA-5	[V ⁴⁺ O(H ₂ O) ₅] ²⁺	[V ⁴⁺ O(H ₂ O) ₅] ²⁺ [V ⁴⁺ O(COOH) ₂]	H ₄ PV ₁ Mo ₁₁ O ₄₀ H ₅ PV ₂ Mo ₁₀ O ₄₀ VO ₂ ⁺ H ₆ PV ₃ Mo ₉ O ₄₀ H ₇ PV ₄ Mo ₈ O ₄₀ H ₈ PV ₅ Mo ₇ O ₄₀ H ₉ PV ₆ Mo ₆ O ₄₀	H ₄ PV ₁ Mo ₁₁ O ₄₀ H ₅ PV ₂ Mo ₁₀ O ₄₀ VO ₂ ⁺ H ₆ PV ₃ Mo ₉ O ₄₀ H ₇ PV ₄ Mo ₈ O ₄₀ H ₈ PV ₅ Mo ₇ O ₄₀ H ₉ PV ₆ Mo ₆ O ₄₀

Reaction conditions: 1 mmol glucose, 0.1 mmol catalyst dissolved in 10 g H₂O, 20 bar O₂, 90 °C, 3 h, 1000 rpm; Conversion, yields and selectivities determined as described in the corresponding section of the experimental part. ^a determined by EPR spectroscopy; ^b determined by ⁵¹V-NMR spectroscopy.

the most active HPA-5 catalyst.

The ⁵¹V NMR spectra (see Fig. 2) are showing the typical peaks for higher V-substituted species such as HPA 4, HPA-5 and HPA 6 (-560 to -620 ppm) as well as the peaks of lower V-substituted species such as HPA-1 (-533 ppm) and HPA-2 (-537 ppm) as well as VO₂⁺/HPA-3 (broad peak at -540 to -560 ppm) [40,51] indicating that higher substituted V-POM-species are the catalytic active species for the glucose oxidation reaction under the applied reaction conditions.

These observations clearly indicate the unique nature of the HPA-5 catalyst leading to an unrivaled activity under the applied mild oxidizing conditions.

For a better overview on the different vanadium species observed in the experiments, Table 2 shows a summary of the different vanadium species resulting from the reaction with glucose under aerobic conditions in aqueous solution.

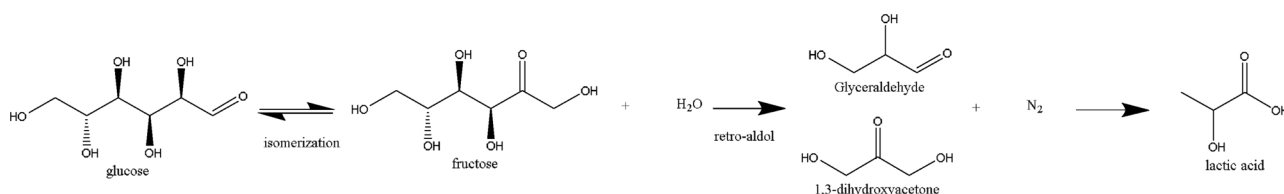
3.2. Catalytic glucose transformation using various V-sources under anaerobic conditions

In the next set of experiments, we wanted to investigate the behavior of different vanadium sources under anaerobic conditions at 20 bar nitrogen atmosphere. Therefore, we used the same V⁴⁺ and V⁵⁺

containing precursors in similar concentrations like mentioned in Table 1. In the beginning, the same reaction conditions despite the reaction atmosphere (nitrogen instead of oxygen) as in the first study were used. However, there was no remarkable catalytic activity detectable for all different vanadium precursors using 90 °C reaction temperature for 3 h reaction time under anaerobic conditions (see ESI, Table S5). Additionally, no changes in the NMR or EPR spectra could be observed. Consequently, we increased the reaction temperature to 160 °C based on a previous study carried out by Tang et al. [14] in order to compare the catalytic performance of diamagnetic and paramagnetic vanadium species under literature-known conditions with a known catalytic reaction pathway. These observations lead us to the assumption that the activation barrier for V catalyzed glucose transformation under anaerobic conditions is much higher than under aerobic conditions that may affect the formation of catalytic active species significantly.

Scheme 3 shows the main reaction pathway from glucose to lactic acid suggested by Tang et al. [14] under anaerobic conditions catalyzed by a VOSO₄ catalyst.

For the glucose transformation reactions under inert atmosphere, we again dissolved 0.1 mmol catalyst in 10 g H₂O and added 1 mmol glucose (0.18 g). The experiments were carried out in the same tenfold



Scheme 3. Main reaction steps for vanadium-catalyzed glucose transformation in aqueous solution under anaerobic conditions [14].

Table 3
Screening of catalysts with different vanadium species for reaction with glucose under N₂-atmosphere at 160 °C.

Entry	Catalyst	Conversion [%]	Yield FA [%]	Yield AA [%]	Yield LA [%]	Yield LevA [%]	Yield HMF [%]	Yield CO ₂ [%]	pH-value before [-]	pH-value after [-]
1	VOSO ₄	47.7	–	1.6	30.2	3.5	12.5	–	3.3	1.9
2	NH ₄ VO ₃	36.2	5.0	2.5	20.5	0.7	7.6	–	6.7	1.8
3	HPA-1	12.5	4.1	3.2	–	2.8	2.4	–	1.5	1.5
4	HPA-5	27.8	9.7	0.8	12.8	–	4.5	–	1.8	1.8

Reaction conditions: 1 mmol glucose, 0.1 mmol catalyst dissolved in 10 g H₂O, 20 bar N₂, 160 °C, 3 h, 1000 rpm; Conversion, yields and selectivities determined as described in the corresponding section of the experimental part.

screening plant with a batch mode reactor setup consisting of ten 20 mL autoclaves in order to neglect influences of different reaction material or up-scaling effects. The reactions were carried out applying increased temperature (160 °C) by keeping all other parameters like stirrer speed, reaction volume and time constant. The results are presented in Table 3.

Contrary to the results obtained under aerobic conditions, all catalysts show higher conversion of glucose due to the higher reaction

temperature under 20 bar nitrogen atmosphere and no CO₂ could be detected in all samples. Regarding the product selectivity, several differences could be observed.

The VOSO₄ shows the highest glucose conversion with 47.7% leading predominantly to lactic acid (LA) with a yield of 30% and the intermediate 5-Hydroxymethylfurfural (HMF) with a yield of 12.5%. Moreover, small amounts with yields < 5% of levulinic acid (LevA), as well as acetic acid (AA) could be detected. The thermally induced glucose isomerisation and dehydration reaction via HMF lead to the obtained reaction products following the mechanisms introduced by Niu et al. [12] and Tang et al. [14] Regarding the spectroscopic investigations, EPR measurements showed again the presence of the same V⁴⁺ species [V⁴⁺O(H₂O)₅]²⁺ (A_{VOSO4}) as before the reaction (Fig. 3 and ESI, Table S1). Surprisingly, its amount has decreased to about 16% of the amount before the reaction (see ESI, Table S1). However, NMR does not resolve any V⁵⁺ signal after the reaction (see ESI, Figure S18), which is reasonable since no oxidising agent was present. In addition to species A_{VOSO4} also an acid-bound vanadyl species [49] B_{VOSO4} could be detected by EPR in very low amounts (Fig. 3 and ESI, Table S1), which might be attributed to a [V⁴⁺O(COOH)₂] species [49,52]. Moreover, these findings suggest that parts of the V⁴⁺ species have been reduced to a V³⁺ species [43], which is expected to be neither NMR nor EPR active (see comment above). Here, at least two V⁴⁺ species are necessary to explain not only these small line splittings, but also the relative intensities of all eight hfi transitions, as it is proven unambiguously by the presented spectral simulations in Fig. 3. Moreover, the pH level after the reaction with 1.9 is slightly lower compared to the one obtained under oxidative conditions (2.1). This is caused by the formation of carboxylic acids (mainly LA) that decrease the pH level of the reaction system.

The V⁵⁺ precursor NH₄VO₃ showed also a medium conversion of 36.2% giving mostly LA (20.5%), HMF (7.6%), FA (5.0%), AA (2.5%) and traces of LevA (0.7%). Interestingly, the EPR spectra showed the same ([V⁴⁺O(H₂O)₅]²⁺) and acid-bound vanadyl species [49,52] than VOSO₄ after the reaction under anaerobic conditions (see ESI, Figure S19, Tables S1 and S2). Furthermore, the total amount of V⁴⁺ has been increased by one order of magnitude (see ESI, Table S2), which might be explained by the increased reaction temperature, leading predominantly to a reduction of the vanadate (V⁵⁺O₃⁻) to the vanadyl (V⁴⁺O²⁺) species. This large EPR derived increase of the amount of acid-bound vanadyl is consistent with the lower pH value after the reaction under anaerobic (1.8) than under aerobic conditions (3.0), which is the largest difference among all vanadium precursors. The ⁵¹V-NMR spectrum did not change qualitatively (see ESI, Figure S20) confirming no change in the V⁵⁺ precursor structure.

HPA-1 shows the lowest conversion rate (X = 12.5%) and a complete different product selectivity as, compared to all other samples, no LA could be detected. Only few amounts of the thermally-induced intermediate HMF (2.4%), its consecutive products FA (4.1%) and LevA (2.4%) as well as a small amount of AA (3.2%) were observed. The EPR spectra (see ESI, Figure S21) confirmed that the same paramagnetic vanadium species as under aerobic conditions are present (see ESI, Figure S13 and Table S3). Like for the NH₄VO₃ precursor, their amounts

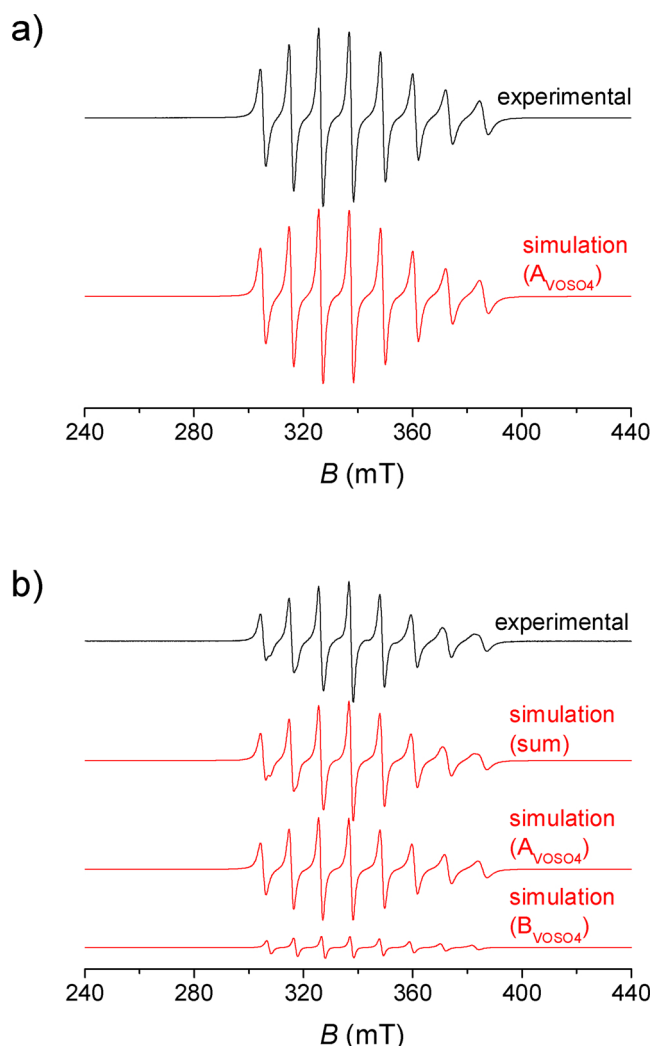


Fig. 3. Experimental (black) and simulated (red) room temperature EPR spectra before (a) and after (b) the reaction of 0.1 mmol VOSO₄ solution with glucose under anaerobic conditions. The experimental signal before the reaction (a) can be simulated by a single species A_{VOSO4} as indicated in the figure. The simulated signal of the spectrum after the reaction (b, sum) is a superposition of two different V⁴⁺ species A_{VOSO4} and species B_{VOSO4} as indicated in the figure. (For interpretation of the references to colour in this figure legend, the reader is referred to the web version of this article).

Table 4

Summary of the different vanadium species resulting from the reaction with glucose under anaerobic conditions determined by EPR and NMR spectroscopy.

Entry	Catalyst	V ⁴⁺ Species before reaction under N ₂ ^a	V ⁴⁺ Species after reaction under N ₂ ^a	V ⁵⁺ Species before reaction under N ₂ ^b	V ⁵⁺ Species after reaction under N ₂ ^b
1	VOSO ₄	[V ⁴⁺ O(H ₂ O) ₅] ²⁺	[V ⁴⁺ O(H ₂ O) ₅] ²⁺ [V ⁴⁺ O(CH ₃ CH ₂ OHCOO) ₂] [V ⁴⁺ O(H ₂ O) ₅] ²⁺	–	–
2	NH ₄ VO ₃	–	[V ⁴⁺ O(CH ₃ CH ₂ OHCOO) ₂] [V ⁴⁺ O(H ₂ O) ₅] ²⁺	[V ⁵⁺ O ₃] [–]	[V ⁵⁺ O ₃] [–]
3	HPA-1	[V ⁴⁺ O(H ₂ O) ₅] ²⁺ VO ²⁺ @ [PV ⁵⁺ Mo ₁₁ O ₄₀] ^{4–}	[V ⁴⁺ O(H ₂ O) ₅] ²⁺ VO ²⁺ @ [PV ⁵⁺ Mo ₁₁ O ₄₀] ^{4–}	[H ₁ PVMo ₁₁ O ₄₀] ^{3–}	[H ₁ PVMo ₁₁ O ₄₀] ^{3–}
4	HPA-5	[V ⁴⁺ O(H ₂ O) ₅] ²⁺	[V ⁴⁺ O(H ₂ O) ₅] ²⁺ [V ⁴⁺ O(COOH) ₂] or [V ⁴⁺ O(CH ₃ CH ₂ OHCOO) ₂]	H ₄ PV ₁ Mo ₁₁ O ₄₀ H ₅ PV ₂ Mo ₁₀ O ₄₀ VO ₂ ⁺ H ₆ PV ₃ Mo ₉ O ₄₀ H ₇ PV ₄ Mo ₈ O ₄₀ H ₈ PV ₅ Mo ₇ O ₄₀ H ₉ PV ₆ Mo ₆ O ₄₀	H ₄ PV ₁ Mo ₁₁ O ₄₀ H ₅ PV ₂ Mo ₁₀ O ₄₀ VO ₂ ⁺ H ₆ PV ₃ Mo ₉ O ₄₀

Reaction conditions: 1 mmol glucose, 0.1 mmol catalyst dissolved in 10 g H₂O, 20 bar N₂, 160 °C, 3 h, 1000 rpm; Conversion, yields and selectivities determined as described in the corresponding section of the experimental part. ^a determined by EPR spectroscopy; ^b determined by ⁵¹V-NMR spectroscopy.

are significantly larger as before the anaerobic reaction and after the reaction under aerobic conditions (see ESI, Table S3), indicating an increased reduction of the V⁵⁺ species due to the larger reaction temperature. This leads us to the assumption that [PV⁵⁺Mo₁₁O₄₀]^{4–} could not be the active species neither for FA formation under aerobic (see Table 1) nor for LA under anaerobic conditions (see Table 3) as it could be resolved only for HPA-1 with this precursor being the only one that did not give both products.

Finally, we investigated the behavior of HPA-5 under anaerobic conditions (Entry 4 in Table 3). The conversion rate for glucose (X = 27.8%) under the applied reaction conditions was somewhat higher than that of HPA-1 but lower than the other precursors VOSO₄ and NH₄VO₃, respectively. Hereby, mostly LA (12.8%) and FA (9.7%) were formed. Again, also thermal-induced reaction products (HMF, LevA and AA) could be detected. Regarding the detected species, NMR (see ESI, Figure S24) gives similar results compared to the aerobic conditions suggesting no qualitative changes of the V⁵⁺ species. As under aerobic conditions, EPR (see ESI, Figure S23) shows the presence of [V⁴⁺O(H₂O)₅]²⁺ (species A_{HPA5}) and acid-bound vanadyl (species B_{HPA5}), but with a significant higher amount due to the absence of any oxygen (see ESI, Table S4). The amount of [V⁴⁺O(H₂O)₅]²⁺ seems to remain constant during the reaction under anaerobic conditions (see ESI, Table S4). Consequently, a partial reduction of the V⁵⁺ species to an acid-bound vanadyl species is indicated.

Obviously, HPA-1 is the only vanadium precursor, which shows under anaerobic conditions no conversion to LA as well as no presence of acid-bound vanadyl after the reaction, whereas the presence of [V⁴⁺O(H₂O)₅]²⁺ after the reaction under anaerobic conditions could be verified for all four vanadium precursors by EPR. This strongly suggests that acid-bound vanadyl might be the predominant active species for the conversion to LA, whereas [V⁴⁺O(H₂O)₅]²⁺ alone does not provide significant catalytic activity. Regarding the ⁵¹V-NMR measurements, no V⁵⁺ species seems to occur significantly when LA is formed.

Table 4 summarizes all identified species by EPR as well as NMR spectroscopy for the conversion of glucose under anaerobic conditions.

4. Conclusions

In this contribution, we investigated the influence of different water-soluble vanadium precursors, namely two commercially available salts (VOSO₄ and NH₄VO₃) as well as two self-synthesized heteropolyacids (HPA-1 and HPA-5) for their catalytic activity in biomass transformation reactions using glucose as a model substrate. Under aerobic conditions (20 bar oxygen atmosphere) at 90 °C, only the HPA-5 precursor showed significant activity for formic acid formation. Using

NMR and EPR spectroscopy, we could clearly prove that the predominant catalytic active species for this transformation are higher substituted heteropolyacids containing V⁵⁺. For glucose transformation under anaerobic conditions (20 bar nitrogen atmosphere) at 160 °C we could show by quantitative EPR that a reduction of V⁵⁺ to V⁴⁺ species takes place for the NH₄VO₃ as well as both heteropolyacid (HPA-1 and HPA-5) precursors independent on the structure of the compounds. Interestingly, the total amount of V⁴⁺ species decreased for VOSO₄ assuming a further reduction to V³⁺ species that are neither detectable by EPR nor by NMR. Hereby, paramagnetic acid-bound vanadyl species formed from the VOSO₄ and NH₄VO₃ as well as the HPA-5 precursor seem to be predominantly responsible for lactic acid formation from glucose under anaerobic conditions. By combining highly efficient detection tools like NMR and EPR for various redox active metals and applying them to complex chemical transformations like biomass oxidation in aqueous media, we hopefully pave the way for more biomass transformation technologies being commercialized in the near future.

Acknowledgments

J. A. and D. V. thank Dr. Nicola Taccardi for performing the ICP measurements. M. M. gratefully acknowledges financial support by the DFG (Deutsche Forschungsgemeinschaft) within the research unit 2433. JA and DV thank the DFG Cluster of Excellence „Engineering of Advanced Materials“ within the EAM Starting Grant SG6. The authors declare no competing financial interests.

Appendix A. Supplementary data

Supplementary material related to this article can be found, in the online version, at doi:<https://doi.org/10.1016/j.apcata.2018.10.030>.

References

- [1] J.N. Chheda, G.W. Huber, J.A. Dumesic, *Angew. Chem. Int. Ed.* **46** (2007) 7164–7183.
- [2] I. Delidovich, K. Leonhard, R. Palkovits, *Energy Environ. Sci.* **7** (2014) 2803–2830.
- [3] C.O. Tuck, E. Perez, I.T. Horvath, R.A. Sheldon, M. Poliakoff, *Science* **337** (2012) 695–699.
- [4] R. Palkovits, K. Tajvidi, A. Ruppert, J. Procelewaska, *Chem. Commun.* **47** (2011) 576–578.
- [5] C. Xu, R.A.D. Arancon, J. Labidi, R. Luque, *Chem. Soc. Rev.* **43** (2014) 7485–7500.
- [6] M. Ruppert, K. Weinberg, R. Palkovits, *Angew. Chem., Int. Ed.* **51** (2012) 2564–2601.
- [7] P. Dhepe, A. Fukuoka, *ChemSusChem* **1** (2008) 969–975.
- [8] R. Wölfel, N. Taccardi, A. Bösmann, P. Wasserscheid, *Green Chem.* **13** (2011) 2759–2763.
- [9] D.M. Alonso, S.G. Wettstein, J.A. Dumesic, *Green Chem.* **15** (2013) 584–595.
- [10] R. Rinaldi, R. Palkovits, F. Schueth, *Angew. Chem. Int. Ed.* **47** (2008) 8047–8050.
- [11] P. Preuster, J. Albert, *Energy Technol.* **6** (2018) 501–509.

- [12] M. Niu, Y. Hou, S. Ren, W. Wang, Q. Zheng, W. Wu, *Green Chem.* 17 (2015) 335–342.
- [13] S.G. Maerten, D. Voß, M.A. Liauw, J. Albert, *ChemistrySelect* 2 (2017) 7296–7302.
- [14] Z. Tang, W. Deng, Y. Wang, E. Zhu, X. Wan, Q. Zhang, Y. Wang, *ChemSusChem* 7 (2014) 1557–15674.
- [15] J. Xu, Y. Zhao, H. Xu, H. Zhang, B. Yu, L. Hao, Z. Liu, *Appl. Catal. B* 154 (2014) 267–273.
- [16] J. Albert, D. Lüders, A. Bösmann, D.M. Guldi, P. Wasserscheid, *Green Chem.* 16 (2014) 226–237.
- [17] S. Shafiee, E. Topal, *Energy Policy* 37 (2009) 181–189.
- [18] S. van de Vyver, J. Geboers, P. Jacobs, B. Sels, *ChemCatChem* 3 (2011) 82–94.
- [19] H. Kobayashi, H. Ohta, A. Fukuoka, *Catal. Sci. Technol.* 2 (2012) 869–883.
- [20] A. Sutton, *Nat. Chem.* 5 (2013) 428–432.
- [21] J. Albert, J. Mehler, J. Tucher, K. Kastner, C. Streb, *ChemistrySelect* 1 (2016) 2889–2894.
- [22] T. Lu, M. Niu, Y. Hou, W. Wu, S. Ren, F. Yang, *Green Chem.* 18 (2016) 4725–4732.
- [23] J.Zhang.M. Sun, X. Liu, Y. Han, *Catal. Today* 233 (2014) 77–82.
- [24] W. Wang, M. Niu, Y. Hou, W. Wu, Z. Liu, Q. Liu, S. Ren, K.N. Marsh, *Green Chem.* 16 (2014) 2614–2618.
- [25] M. Wang, J. Lu, X. Zhang, L. Li, H. Li, N. Luo, F. Wang, *ACS Catal.* 6 (2016) 6086–6090.
- [26] M. Ammam, *J. Mater. Chem. A* 1 (2013) 6291–6312.
- [27] W. Deng, Q. Zhang, Y. Wang, *Dalton Trans.* 41 (2012) 9817–9831.
- [28] S. Wang, G. Yang, *Chem. Rev.* 115 (2015) 4893–4962.
- [29] I.V. Kozhevnikov, *Chem. Rev.* 98 (1998) 171–198.
- [30] H.N. Miras, J. Yan, D.L. Long, L. Cronin, *Chem. Soc. Rev.* 41 (2012) 7403–7430.
- [31] E.G. Zhizhina, Y.A. Rodikova, V.N. Parmon, *ChemistrySelect* 2 (2017) 4686–4690.
- [32] J. Reichert, B. Brunner, A. Jess, P. Wasserscheid, J. Albert, *Energy Environ. Sci.* 8 (2015) 2985–2990.
- [33] J. Albert, P. Wasserscheid, *Green Chem.* 17 (2015) 5164–5171.
- [34] J. Albert, R. Wölfel, A. Bösmann, P. Wasserscheid, *Energy Environ. Sci.* 5 (2012) 7956–7962.
- [35] J. Albert, *Faraday Discuss.* 202 (2017) 99–109.
- [36] J. Reichert, J. Albert, *ACS Sustain. Chem. Eng.* 5 (2017) 7383–7392.
- [37] M.H. Levitt, *Spin Dynamics. Basics of Nuclear Magnetic Resonance*, (2008).
- [38] J.D. Satterlee, *Concepts Magn. Reson.* 2 (1990) 119–129.
- [39] N.M. Atherton, *Principles of Electron Spin Resonance*, Ellis Horwood; PTR Prentice Hall, New York, 1993.
- [40] V.F. Odyakov, E.G. Zhizhina, *React. Kinet. Catal. Lett.* 95 (2008) 21–29.
- [41] R.K. Murmann, K.C. Giese, *Inorg. Chem.* 17 (1978) 1160–1165.
- [42] B. Bertleff, J. Claußnitzer, W. Korth, P. Wasserscheid, A. Jess, J. Albert, *Energy Fuels* 32 (2018) 8683–8688.
- [43] S.K. Hanson, R.T. Baker, J.C. Gordon, B.L. Scott, A.D. Sutton, D.L. Thorn, *JACS* 131 (2009) 428–437.
- [44] M. Tregenna-Piggott, *Inorg. Chem.* 38 (1999) 5928–5929.
- [45] M. Weckhuysen, D.E. Keller, *Catal. Today* 78 (2003) 25–46.
- [46] S.E.O. Donnell, M.T. Pope, *J. Chem. Soc.* 1 (1976) 2290–2297.
- [47] S. Hayashi, K. Hayamizu, *Bull. Chem. Soc. Jpn.* 63 (1990) 961–963.
- [48] C.V. Grant, W. Cope, J.A. Ball, G.G. Maresch, B.J. Gaffney, W. Fink, R.D. Britt, *J. Phys. Chem. B* 103 (1999) 10627–10632.
- [49] K. Wüthrich, *Helv. Chim. Acta* 48 (1965) 779–790.
- [50] R. Bayer, C. Marchal, F.X. Liu, A. Tézé, G. Hervé, *J. Mol. Catal. A* 110 (1996) 65–76.
- [51] E.G. Zhizhina, V.F. Odyakov, M.V. Simonova, *Kinet. Catal.* 49 (2008) 773–781.
- [52] S. Berto, P.G. Daniele, E. Prenesti, E. Laurenti, *Inorg. Chim. Acta* 363 (2010) 3469–3478.
- [53] S. Stoll, A. Schweiger, *J. Magn. Reson.* 178 (2006) 42–55.
- [54] M. Gutjahr, J. Hoentsch, R. Böttcher, O. Storcheva, K. Köhlrt, A. Pöpl, *JACS* 126 (2004) 2905–2911.
- [55] A. Pöpl, P. Manikandan, K. Köhler, P. Maas, P. Strauch, R. Böttcher, D. Goldfarb, *JACS* 123 (2001) 4577–4584.
- [56] J. Li, D.J. Ding, L. Deng, Q.X. Guo, Y. Fu, *ChemSusChem* 5 (2012) 1313–1318.